이학석사 학위논문

The effect of vegetation feedback on the regional precipitation in the eastern part of Mongolian Plateau

몽골 고원의 동부 지역에서

식생 피드백이 강수량에 미친 영향

2019년 8월

서울대학교 대학원

지구환경과학부

김익호

Abstract

The effect of vegetation feedback on the regional precipitation in the eastern part of Mongolian Plateau

Ikho Kim

School of Earth and Environmental Sciences

The Graduate School of Seoul National University

The atmosphere-vegetation feedback is one of the phenomenon that produces large uncertainty in climate studies. In the past, researches on vegetation feedback were mainly focused on the forests rather than the non-forest area including dry land which occupies 40% of the Earth’s land surface. In dry land, precipitation and soil moisture are strongly coupled, and vegetation modulates the stability of this coupling. Because the precipitation–vegetation feedback in dry land can be either positive or negative depending on region, timing, and magnitude of the initial perturbation, it is needed to be discussed focusing on individual cases. In this thesis, the role of vegetation feedback on the ongoing increasing trend of precipitation in the eastern part of Mongolian Plateau (EMP) was analyzed using statistical analysis

with observation dataset and regional climate model simulation.

In the EMP region, the normalized difference vegetation index (NDVI) has increased 40% in recent ten years compared to its climatological mean. And the precipitation has increased 60% for the same period. The previous research has claimed that the increased precipitation has led the increase of vegetation activity. However, when the fundamental meteorological fields were examined, no sign of large-scale circulation change was shown that seems to be enough to force the recent precipitation increase. Instead, the dry and moist static stability in the lower atmosphere, which had always been similar in decadal scale variability over the last 50 years, have been observed to split from the mid-2000s. Thus, there was a reasonable doubt that the moisture flux near surface was changed and that change has led the recent increasing trend of precipitation since mid-2000s. Also, the main modulator of surface moisture flux was thought to be the increased activity of vegetation after 2007.

Regional climate model experiments were conducted to verify the effect of vegetation activity on local precipitation using The Weather Research and Forecasting (WRF) model. The main driver of recent increasing trend of growing season precipitation in the EMP region was the increased moisture supply from the surface through evapo-transpitation rather than convective motion of the

atmosphere. When removed the effect of increased vegetation activity by fixing the leaf area index (LAI) as the value of 2007 which was the lowest in the recent decade, the increased trend of latent heat flux from the land surface was significantly reduced.

When the results of the observation data analysis and the regional climate model simulation were synthetically considered, it is reasonable to conclude that vegetation feedback has been playing significant role on the observed recent decade's increasing trend of precipitation in EMP region. No evidence has been found that the changes of large-scale circulation have led the precipitation increase. On the other hand, the increasing moisture supply from the land surface into the atmosphere was observed. Also, the result of regional climate model simulation showed that this increasing trend of moisture flux has been mainly due to the increase of transpiration by the vegetation. The overall mechanism was that the steady increase of vegetation activity over the period from 2007 to 2015 had increased the amount of transpiration, so the amount of moisture supplied to the lower atmosphere has increased, resulted in the increase of local precipitation.

Keywords: climate system, atmosphere-vegetation feedback, dry land,
Mongolian plateau, precipitation, evapo-transpiration
Student Number: 2016-20411

Contents

Abstract i

Contents iv

List of figures vi

1. Introduction 1

2. Data and Methods 5

2.1 Data 5

2.2 Statistical Analysis. 9

2.3 Model description and experiment design. 11

3. Analysis of observation data 13

3.1 Recent change of precipitation and vegetation activity 13

3.2 Background meteorological fields 19

3.3 Static stability of lower atmosphere 23

4. Regional climate model simulation 26

4.1 Model validation of precipitation simulation 26

4.2 Result of model experiment with modified vegetation activity 30

5. Concluding remarks 34

Reference 36

국문 초록 41

List of figures

Figure 1 Example of temporal interpolation of MODIS LAI dataset. Small blue dots indicate horizontally interpolated 8-days composited LAI data. Dashed blue line indicates smoothed and continuous seasonal cycle curve, applied discrete Fourier transform and discarded signal of period under 40-days. Big purple dots indicate monthly representative value.

Figure 2 The linear trend of growing season averaged GIMMS NDVI3gv1 from 1994 to 2007(a) and from 2007 to 2015(b). The black dots indicate 95% statistical significant ($p<0.05$). For the past period, EMP region showed decreasing trend of vegetation activity. However, after 2007, it turned out to be increasing trend.

Figure 3 The linear trend of growing season accumulated CMAP(precipitation) from 1994 to 2007(a) and from 2007 to 2015(b). The black dots indicate 95% statistical significant ($p<0.05$). For the past period, northern boundary of Gobi Desert showed significant decreasing trend of growing season precipitation and EMP region showed decreasing trend but not significant. However, after 2007, EMP region turned out to be increasing trend.

Figure 4 Seasonal cycle of two separated 3-year period of NDVI(a) and precipitation(b). Green line is averaged from recent 3-years period (2013-2015)

and blue line is for past 3-years period (2006-2008). Both NDVI and precipitation showed consistent increase for all month in growing season.

Figure 5 Time series of growing season averaged NDVI(a) and growing season accumulated precipitation(b) for past 30-years period (1986-2015). Dashed line is low pass filtered, which is removed the variation with a period of less than 5 years. Both NDVI and precipitation show increasing trend after 2007. Especially for NDVI, recent value is extra-ordinary compared to past period.

Figure 6 Linear trend of horizontal moisture flux on the surface(a) and on the 700 hPa isobaric surface from 2007 to 2015. Only the vectors which have 95% statistical significance ($p<=0.05$) either east-west or south-north are shown as thick arrows. Near surface, increase of moisture influx from the eastern coast of Russia to the land area, but it does not reach inside the EMP region. On the 700 hPa isobaric surface, westward outflow along the northern boundary of the EMP region, rather the inflow to the EMP region, is shown.

Figure 7 Linear trend of air temperature(a) and pressure(b) on the surface from 2007 to 2015. Black dots are indicating 95% statistical significance ($p<=0.05$). Decreasing trend of surface temperature in Mongolia and EMP region is shown but is not statistically significant except the 2 grid points centered in mid Mongolia.

Figure 8 Linear trend of air temperature(a) and geopotential height (b) on the 500 hPa isobaric surface from 2007 to 2015. No grid shows 95% statistical significance. Geopotential height in Mongolia shows decreasing trend, which is dynamically consistent with the surface temperature, but the statistical significance is not high.

Figure 9 The linear trend of growing season averaged moist(a) and dry(b) static stability between 1000hPa and 850hPa isobaric surface from 2006 to 2015. The black dots indicate statistical significant ($p<0.05$). Plot (c) is showing low pass filtered time series of moist (blue line) and dry (red line) static stability, averaged upon growing season and the EMP region. Dashed lines are showing law data that is not applied the low pass filter.

Figure 10 The vertical profile of specific humidity(a) and temperature(b) averaged up the EMP region. The blue lines indicate the averaged value of 3-year period from 2006 to 2008, and the green lines are for 2013 to 2015.

Figure 11 The growing season accumulated total precipitation, averaged from 2007 to 2015, ERA-interim(a) and WRF model simulation result(b). The mean bias (WRF-ERAi) is about 134mm and WRF result showed little bit larger spatial heterogeneity. The overall spatial pattern is reasonable with cosine similarity about 0.986.

Figure 12 The growing season accumulated large scale precipitation, averaged from 2007 to 2015, ERA-interim(a) and WRF model simulation result(b). The mean bias (WRF-ERAi) is about 35mm. The overall spatial pattern is reasonable with cosine similarity about 0.980.

Figure 13 The growing season accumulated convective precipitation, averaged from 2007 to 2015, ERA-interim(a) and WRF model simulation result(b). The mean bias (WRF-ERAi) is about 99mm. In spite of the over simulation, the spatial pattern is reasonable with cosine similarity about 0.982.

Figure 14 Linear trend of growing season accumulated latent heat flux at the surface of control run(a), experimental run(b) and the difference(c). Experimental run only considers the change due to background meteorological field, without the effect of vegetation, so (c) shows the amount of effect from vegetation change.

Figure 15 Linear trend of growing season accumulated large scale precipitation of control run(a), experimental run(b) and the difference(c). Experimental run considers the change of precipitation only due to background meteorological field, without the effect of vegetation, so (c) shows the amount of effect from vegetation change.

Figure 16 Linear trend of growing season accumulated convective precipitation of control run(a), experimental run(b) and the difference(c). Experimental run considers the change of precipitation only due to background meteorological field, without the effect of vegetation, so (c) shows the amount of effect from vegetation change.

1. Introduction

Vegetation activities and the regional climate are influenced by each other in various physical or chemical mechanisms. When we decompose the relationship between two systems, climate and vegetation, into networks of individual physical or chemical variables, we can find out various kinds of closed circuit feedback loops. Unlike simple two-step feedback, closed circuit feedback loop can reinforce the initial perturbation and make it as a longer lasting trend. Thus, the detailed understanding about theses feedback loops is very important for accurate prediction of long-term climate change (Alkama & Cescatti, 2016; Bonan, 2008; S. J. Jeong et al., 2014; Richardson et al., 2013).

In the past when climate change researches was mainly focusing on rising temperature and its first-order consequences, the researches on vegetation feedback had been held mostly on temperature sensitive areas, such as temperate or boreal forest (Bonan, 2008; Ollinger et al., 2008). For the rest of the world, only some fragmented researches about the forcing of vegetation to the atmosphere or the response of vegetation to recent climate change have been discussed (Elmendorf et al., 2012; Myers-Smith et al., 2011). Among the rest, dry land occupies about 40 percent of the Earth's land surface (Henninger, 2002). This value is more than two times larger than the sum of temperate and boreal forest (Bonan, 2008). In addition, according to recent studies about terrestrial water balance, dry land is predicted to be larger in the future along the climate change (Huang, Guan, & Wang, 2015; Park et al., 2017). Thus, there is a growing need to study about vegetation feedback in dry land.

In dry land, moisture is the key variable which modulate the relationship between climate and vegetation (Henninger, 2002). Water limited vegetation responds very sensitively and consistently to the variability of precipitation; the more precipitation, the more vegetation growth. Unlike the simple pathway from precipitation to vegetation, the feedback from vegetation to precipitation is much complex. Most of inland dry areas have high precipitation recycling ratio, which means precipitation depends on local evapotranspiration. In this environment, the soil acts as a land memory by storing the precipitated water for a while and returning it to the atmosphere. Because of this memory, an initial perturbation, such as unusual large amount of precipitation, can be long lasting and sometimes amplifying. This is called soil moisture – precipitation coupling. Vegetation modulate this coupling by enhancing the transferring of moisture in the soil to the atmosphere through water absorption by root and transpiration by shoot. In some circumstance, this enhancement reduces surface runoff and infiltration to the deep groundwater. It means, the moisture is made to be staying in particular region circulating between atmosphere and soil inside the region. On the other hand, if the vegetation enhances evapotranspiration too much, it volatizes the land memory of moisture perturbation. Overall, feedback between precipitation and dry land vegetation can be either positive or negative (Lemordant, Gentine, Swann, Cook, & Scheff, 2018; Los et al., 2006; Ridder, 1998; Scheffer, Holmgren, Brovkin, & Claussen, 2005). Because of this complexity and inconsistency, researches about dry land vegetation feedback have to be held focusing on individual cases.

The eastern part of Mongolian Plateau (EMP), which comprises the eastern Mongolia and north-eastern China, is a semi-arid region with around 300~500 mm of annual precipitation and occupied mainly by grassland with sparse woody plants. The EMP was reported as a desertification area since mid-1990s (S.-J. Jeong, Ho, Brown, Kug, & Piao, 2011). After that, recent studies have shown that vegetation in this region has returned to increasing trend after reaching its lowest point in 2007 (Zhao et al., 2015). Both studies have also reported the decreasing / increasing trend of growing season precipitation in each period and explained the changes of vegetation amount as a consequence of precipitation. However, there can be a reasonable doubt that vegetation has been playing a subjective role on recent trend rather than been just a passive variable tied to precipitation.

The objective of this thesis is to analyze in detail about recent trends of precipitation and vegetation in EMP region, to verify whether vegetation feedback has played an active role, and to identify what kind of feedback has been done and the mechanism. Various type of statistical analysis including linear regression, time series analysis and low pass filter using satellite observation data and reanalysis data was performed for the first object. Also, a few sets of regional climate model experiment were performed with artificially manipulated data field of vegetation. Each result was analyzed and compared focusing on regional water cycle.

2. Data and Methods

2.1 Data

As an indicator of vegetation activity, the 3rd generation version 1 of normalized difference vegetation index (NDVI3gv1) created by Global Inventory Modeling and Mapping Studies (GIMMS) from satellite observation data of advanced very high-resolution radiometers (AVHRR) was used. The NDVI3gv1 has a spatial resolution of 1/12 degrees and bi-monthly time resolution. To minimize the effect of meteorological contamination on satellite observation, the highest value is used as the representative value during each half-month period (Tucker et al., 2005). In order to compare the vegetation activity with other climate variables, for the spatial pattern analysis, linear regression analysis, and correlation analysis, gridded data which is aggregated into 0.5°x0.5° spatial resolution by averaging 6x6 grids of raw data for each 0.5°x0.5° grid is used.

For analyzing decadal trend and seasonal cycle of precipitation, standard monthly Climate Prediction Center (CPC) Merged Analysis of Precipitation (CMAP) made by NOAA was used. Gauge data and 5 kinds of satellite observation; Geostationary Operational Environmental Satellite (GOES) Precipitation Index (GPI), Outgoing Longwave Radiation (OLR) Precipitation Index (OPI), Special Sensor Microwave/Imager (SSM/I) scattering, SSM/I emission, and Microwave

Sounding Unit (MSU), are used for CMAP dataset. The spatial resolution of CMAP dataset is 2.5°x2.5° (Xie, Arkin, Xie, & Arkin, 1997).

To verify if there was a change in the large scale atmospheric circulation that might have affected precipitation amount, monthly mean data of air temperature, geopotential height, specific humidity, vertical and horizontal wind which are included in National Centers for Environmental Prediction (NCEP) / National Center of Atmospheric Research (NCAR) reanalysis 1 dataset was used. The spatial resolution of NCEP/NCAR reanalysis 1 dataset is 2.5°x2.5° (Kalnay et al., 1996).

For the initial and boundary condition of regional climate model experiment, European Centre for Medium-Range Weather Forecasts (ECMWF) ERA-interim dataset was used. ERA-interim is a reanalysis dataset which has about 0.7°x0.7° spatial resolution and 6-hourly temporal resolution (Dee et al., 2011). Monthly accumulated ERA-interim dataset of large scale and convective precipitation was also used for the validation of climate model simulation result.

Moderate Resolution Imaging Spectroradiometer (MODIS) Leaf Area Index (LAI) was used for terrestrial input data of climate model experiment. Among types of MODIS LAI datasets, MCD15A2H is used which has 500m x 500m spatial resolution and 8-days temporal resolution, retrieved from both MODIS Terra and Aqua satellite observation. For each 8-days period, maximum value is chosen for the representative value in order to minimize the effect of meteorological contamination on satellite observation (Myneni, Knyazikhin, & Park, 2015). In this research, spatial resolution is aggregated into 30km x 30km by using bilinear interpolation method. For the use as an input data of regional climate model, temporal resolution is transformed into monthly. For each year and each grid, discrete Fourier transform is applied using data from 73rd~80th day of year (DOY) (14, March) to 321st~318th DOY (17, November). By discarding variation which has period under 40-days, smoothed and continuous seasonal cycle curve is obtained. 16th day's value of each month is chosen as a monthly representative value (fig1).

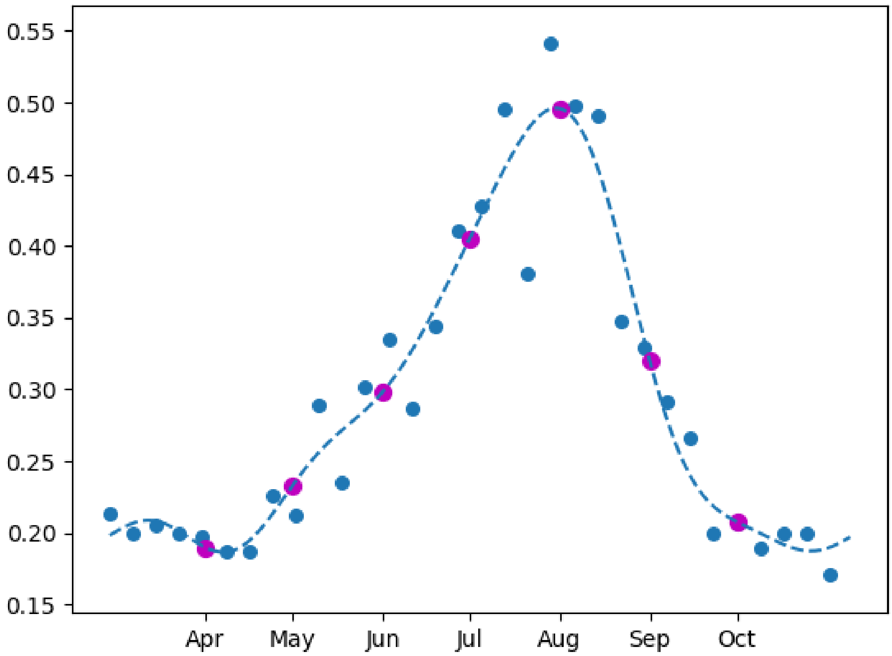

Figure 1 Example of temporal interpolation of MODIS LAI dataset. Small blue dots indicate horizontally interpolated 8-days composited LAI data. Dashed blue line indicates smoothed and continuous seasonal cycle curve, applied discrete Fourier transform and discarded signal of period under 40-days. Big purple dots indicate monthly representative value.

2.2 Statistical Analysis.

The NDVI and CMAP data were averaged from May to September, which is the growing season of EMP region, to obtain annual representative value. For each grid point, a linear regression was applied to the 9 year values from 2007 to 2015 in order to identify the spatial distribution of the magnitude of linear trend and its statistical significance. After this analysis, the region of 115°E-125°E and 45°N-50°N, which showed most significant changes of NDVI and precipitation in recent decade, was chosen for seasonal cycle and time series analysis. Using data of 30 years from 1986 to 2015, growing season averaging and spatial averaging was applied and obtained the time series of inter-annual variability of vegetation amount and precipitation. For making clear of decadal scale variability, the low pass filter was applied to remove signals with periods less than 5 years using discrete Fourier transform. In order to confirm the change of the seasonal cycle, the average seasonal cycle for three years from 2006 to 2008 and the average seasonal cycle for three years from 2013 to 2015 were calculated and compared.

In order to identify the main atmospheric driver of recent precipitation increase, the moist and dry static stability between surface (2m) and 700hPa was calculated using air temperature, geopotential height and specific humidity of NCEP reanalysis 1 dataset for both monthly and growing season averaged field. For specific humidity, horizontal spatial averaged vertical profile was calculated for averaged value of three years from 2006 to 2008 and from 2013 to 2015 and compared same as other variables.

2.3 Model description and experiment design.

The Weather Research and Forecasting (WRF) model is used for regional climate simulation. The spatial resolution was 30km x 30km. 90 x 80 grid points are simulated centered at 47°N and 122°E. All results were analyzed with mean of 5 ensemble runs. For each ensemble, starting date of simulation was varying from April 21st to April 25th and end date was September 30th, same for every run. Sliced run was done, repeating for 9 years from 2007 to 2015. The simulation result was analyzed using only from May 1st to September 30th for every ensemble. Also, for the boundary of simulation region, 15 grids were cut out for all four sides, in order to reducing the effect of simulation error at the boundary area. WRF Single-moment 6-class scheme for cloud microphysics, CAM3 scheme for longwave and shortwave radiation, and Kain-Fritsch scheme for cumulus parameterization are used for atmospheric physics simulation. For the land surface physics simulation, Noah Land Surface Model is used. Sea surface temperature (SST) was updated for every 6 hours and LAI was updated for every day.

For control run, MODIS LAI is used for input data of vegetation without any modification except horizontal and temporal interpolation. For the experimental run, LAI data of 2007, which was the lowest value in recent period, was used for all years in experimental period (from 2007 to 2015), to identify whether the trend of precipitation is maintained when the vegetation doesn't correspond to precipitation change. The output precipitation, evapotranspiration and moisture flux data were analyzed and compared between control and experimental run.

3. Analysis of observation data

3.1 Recent change of precipitation and vegetation activity

For the period from 1994 to 2007, the northern and eastern side of Gobi Desert had been shown decreasing trend of growing season averaged NDVI, consistent result with Jeong *et al.* 2014. However, for the period from 2007 to 2015, along the northern and eastern boundary of Gobi Desert, strong increasing trend of growing season averaged NDVI was shown and the strongest and largest signal was at the EMP region (fig2). The growing season total precipitation showed similar pattern with NDVI for the period from 1994 to 2007. After 2007, the increasing trend of precipitation was shown in the Northern China, the eastern area of EMP region (fig3). Both NDVI and precipitation, the slope is about 7~8% of climatology per year, it means about 60% increase was showed for 9 years. Focusing on seasonal cycle, both NDVI and precipitation of recent three years (2013~2015) was showed significant increase for all months in growing season compared to past 3-year period (2006~2008) (fig4). This means the increasing trend of growing season averaged NDVI and growing season accumulated precipitation was not because of phenological change or expansion of summer. When the time series of the last 30-year period was checked, the recent increasing of NDVI was shown to be extra-ordinary, out of the range of variability of the past.

This out-ranged increasing might have changed the regime of vegetation feedback recently. On the other hand, precipitation increasing is relatively small, within the range of the past variability (fig5).

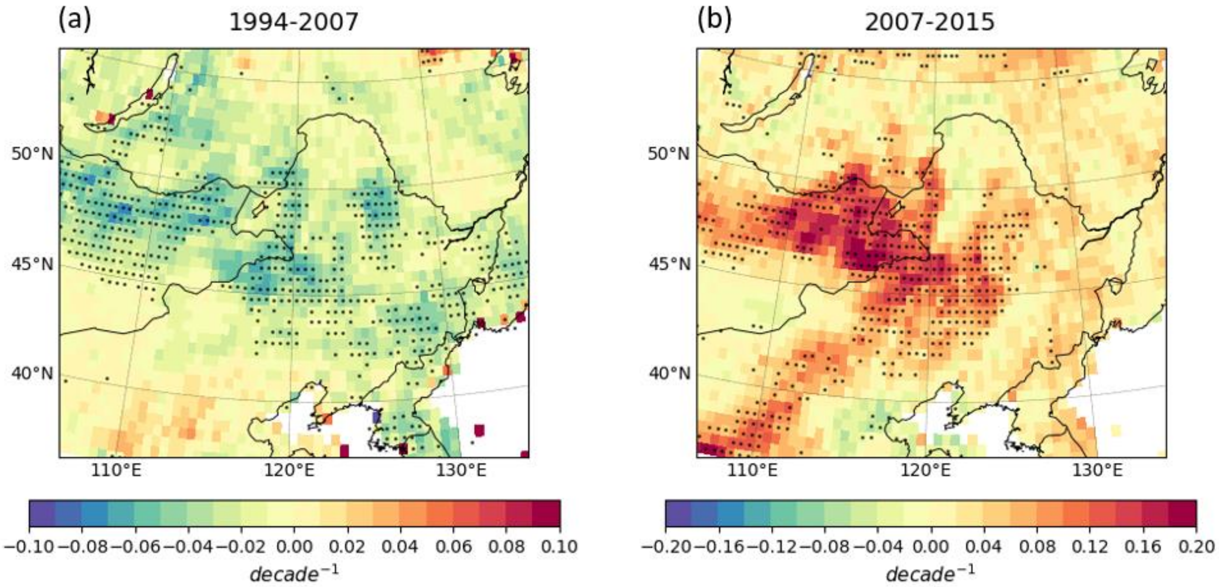

Figure 2 The linear trend of growing season averaged GIMMS NDVI3gv1 from 1994 to 2007(a) and from 2007 to 2015(b). The black dots indicate 95% statistical significant ($p<0.05$). For the past period, EMP region showed decreasing trend of vegetation activity. However, after 2007, it turned out to be increasing trend.

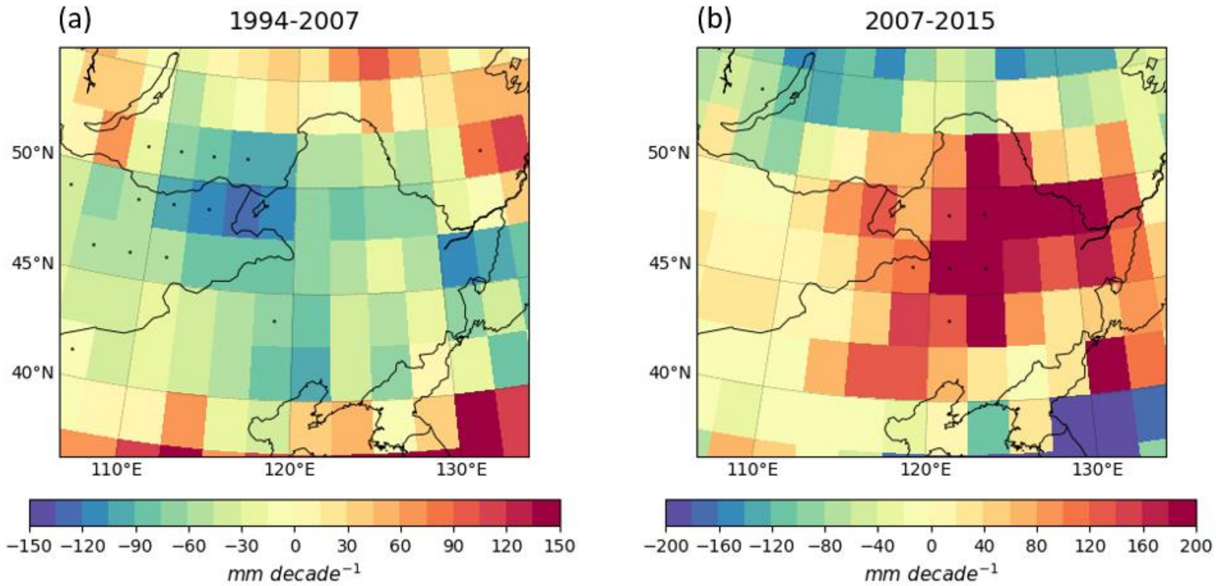

Figure 3 The linear trend of growing season accumulated CMAP (precipitation) from 1994 to 2007 (a) and from 2007 to 2015 (b). The black dots indicate 95% statistical significant ($p<0.05$). For the past period, northern boundary of Gobi Desert showed significant decreasing trend of growing season precipitation and EMP region showed decreasing trend but not significant. However, after 2007, EMP region turned out to be increasing trend.

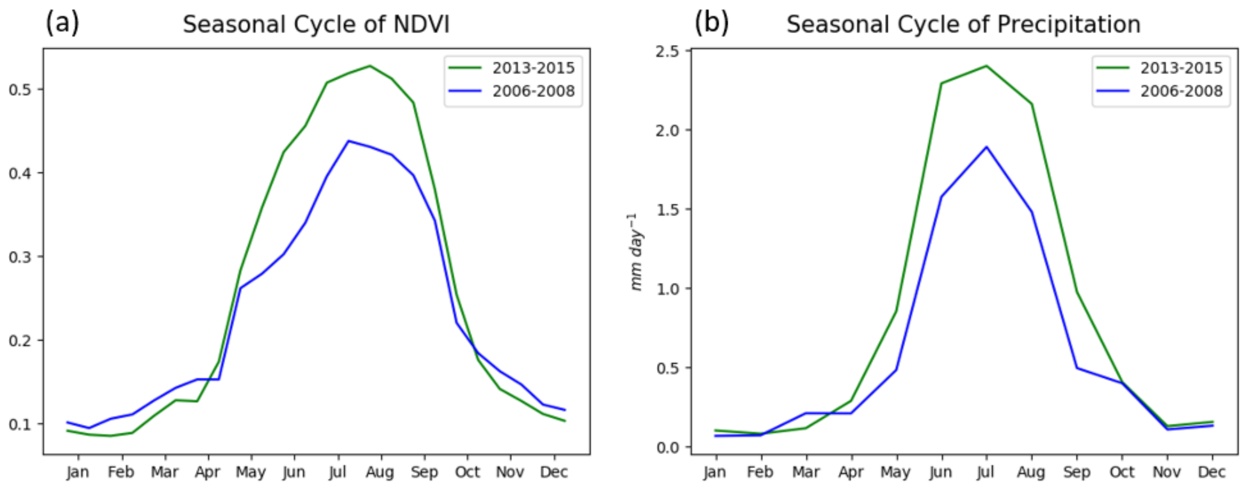

Figure 4 Seasonal cycle of two separated 3-year period of NDVI (a) and precipitation (b). Green line is averaged from recent 3-years period (2013-2015) and blue line is for past 3-years period (2006-2008). Both NDVI and precipitation showed consistent increase for all month in growing season.

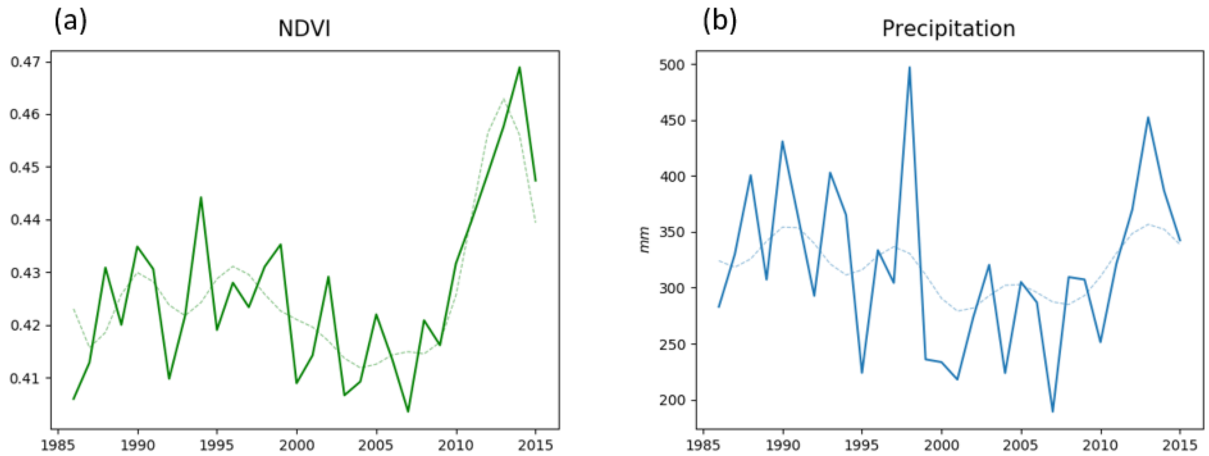

Figure 5 Time series of growing season averaged NDVI (a) and growing season accumulated precipitation(b) for past 30-years period (1986-2015). Dashed line is low pass filtered, which is removed the variation with a period of less than 5 years. Both NDVI and precipitation show increasing trend after 2007. Especially for NDVI, recent value is extra-ordinary compared to past period.

3.2 Background meteorological fields

Among the possible cause of recent precipitation increase, the change of horizontal moisture flux was checked. Near the surface layer, increasing inflow of moisture flux from the eastern coast of Russia was shown but it didn't deeply come into the EMP region (fig6, a). On the 700 hPa isobaric surface, moisture influx to the EMP region was not shown. Rather, westward outflow along the northern boundary of EMP region was shown (fig6, b). When checked the most fundamental meteorological variables; temperature and pressure on the surface(fig7) and on the 500 hPa isobaric surface(fig8), almost no grid point was shown statistically significant linear trend.

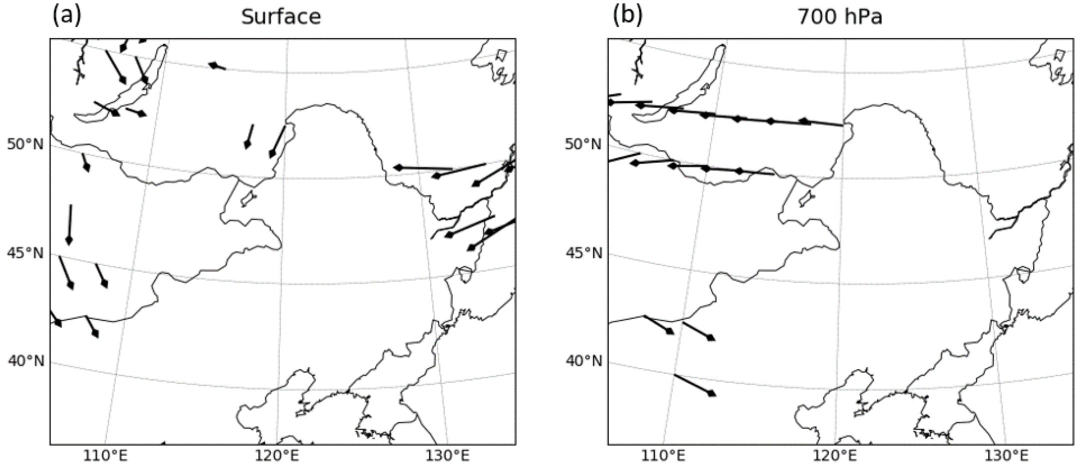

Figure 6 Linear trend of horizontal moisture flux on the surface (a) and on the 700 hPa isobaric surface (b) from 2007 to 2015. Only the vector which has 95% statistical significance ($p<0.05$) either east-west or south-north is shown as thick arrows. Near surface, increase of moisture influx from the eastern coast of Russia to the land area, but it does not reach inside the EMP region. On the 700 hPa isobaric surface, westward outflow along the northern boundary of the EMP region, rather the inflow to the EMP region, is shown.

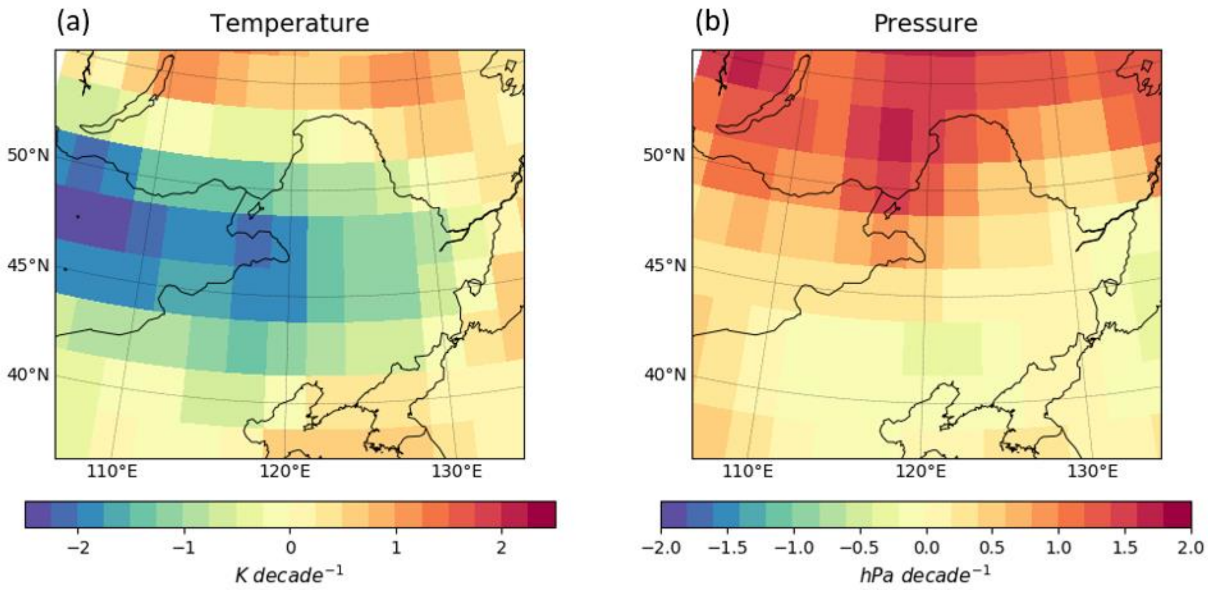

Figure 7 Linear trend of air temperature (a) and pressure (b) on the surface from 2007 to 2015. Black dots are indicating 95% statistical significance ($p<0.05$). Decreasing trend of surface temperature in Mongolia and EMP region is shown but is not statistically significant except the 2 grid points centered in mid Mongolia.

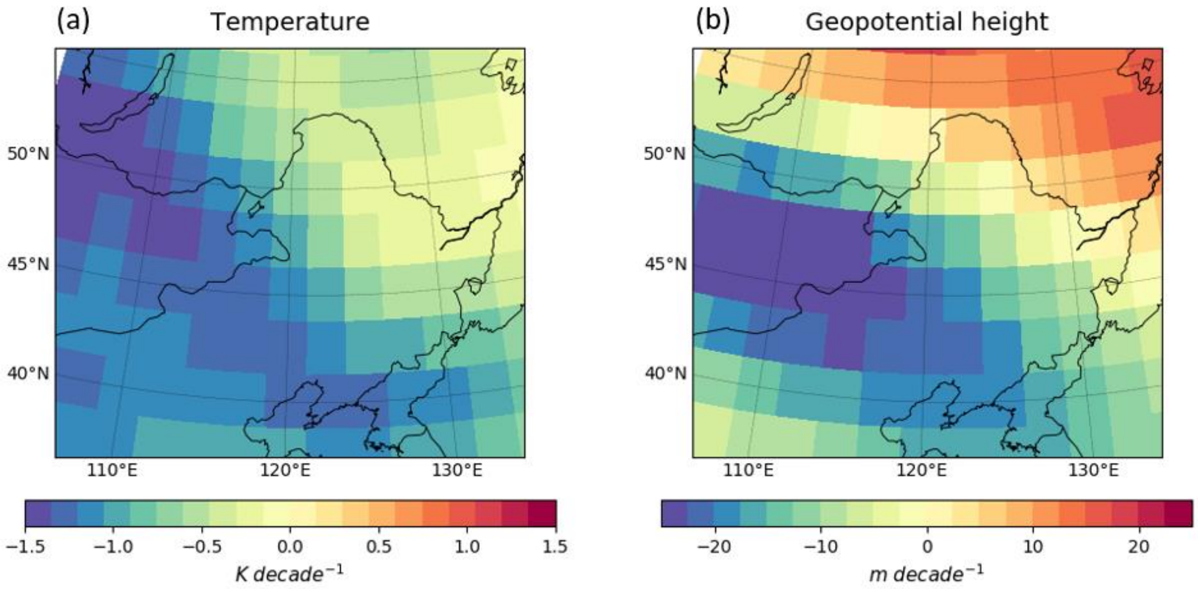

Figure 8 Linear trend of air temperature (a) and geopotential height (b) on the 500 hPa isobaric surface from 2007 to 2015. No grid shows 95% statistical significance. Geopotential height in Mongolia shows decreasing trend, which is dynamically consistent with the surface temperature, but the statistical significance is not high.

3.3 Static stability of lower atmosphere

The lower atmosphere moist static stability during the growing season between the surface (2m) and 700hPa isobaric surface was showed to be increased very steeply in all around of Mongolia and north-eastern China (fig9, a). However, the dry static stability only increased central Mongolia which is much drier that the EMP region and north-eastern China (fig9, b). For EMP region, when checking the low pass filtered time series of last 30 years, the long term, multi decadal trend was increasing for last 30 years for dry static stability, but the moist static stability had started to decrease very significantly in recent 10 years (fig9, c). This means the moisture near land surface is increasing. This change was also appeared in the vertical profile of specific humidity in the EMP region (fig10, a). The air temperature, didn't show any difference between 2006-2008 and 2013-2015 at the 1000hPa isobaric surface, unlike the upper layers (fig10, b). It can be suspected that the increased latent heat flux is compensating the increase of lower level energy due to global warming.

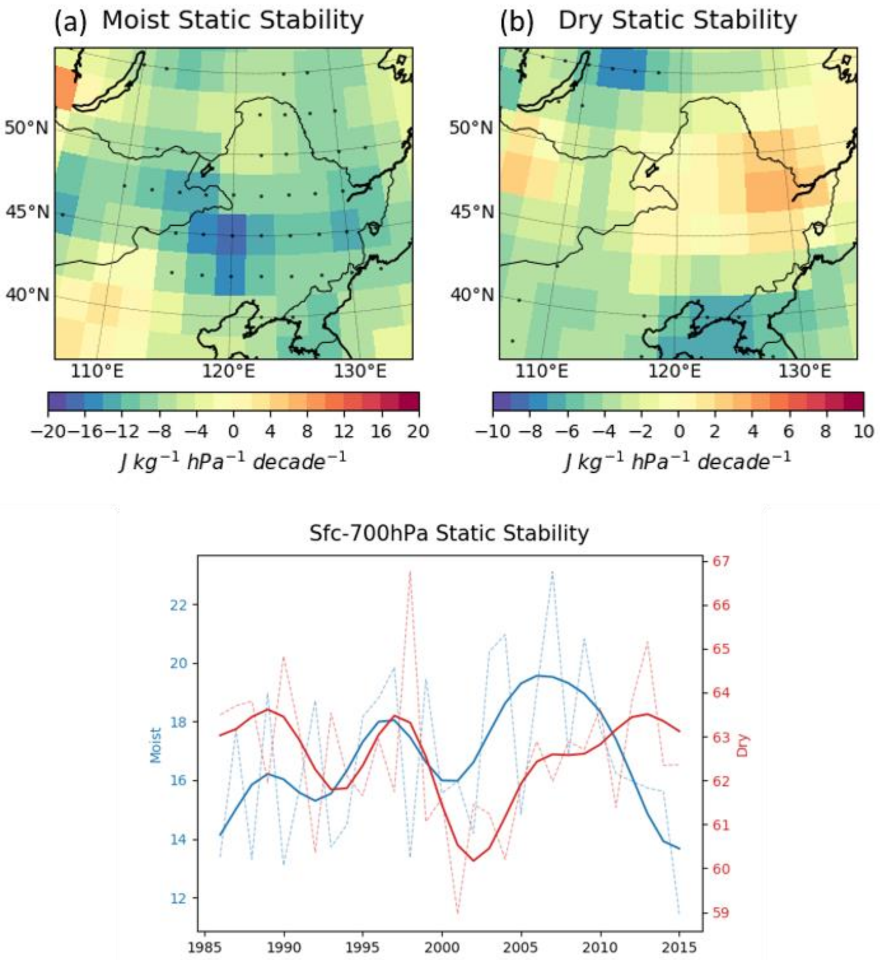

Figure 9 The linear trend of growing season averaged moist (a) and dry (b) static stability between surface and 700hPa isobaric surface from 2007 to 2015. The black dots indicate statistical significant ($p<0.05$). Plot (c) is showing low pass filtered time series of moist (blue line) and dry (red line) static stability, averaged upon growing season and the EMP region. Dashed lines are showing law data that is not applied the low pass filter.

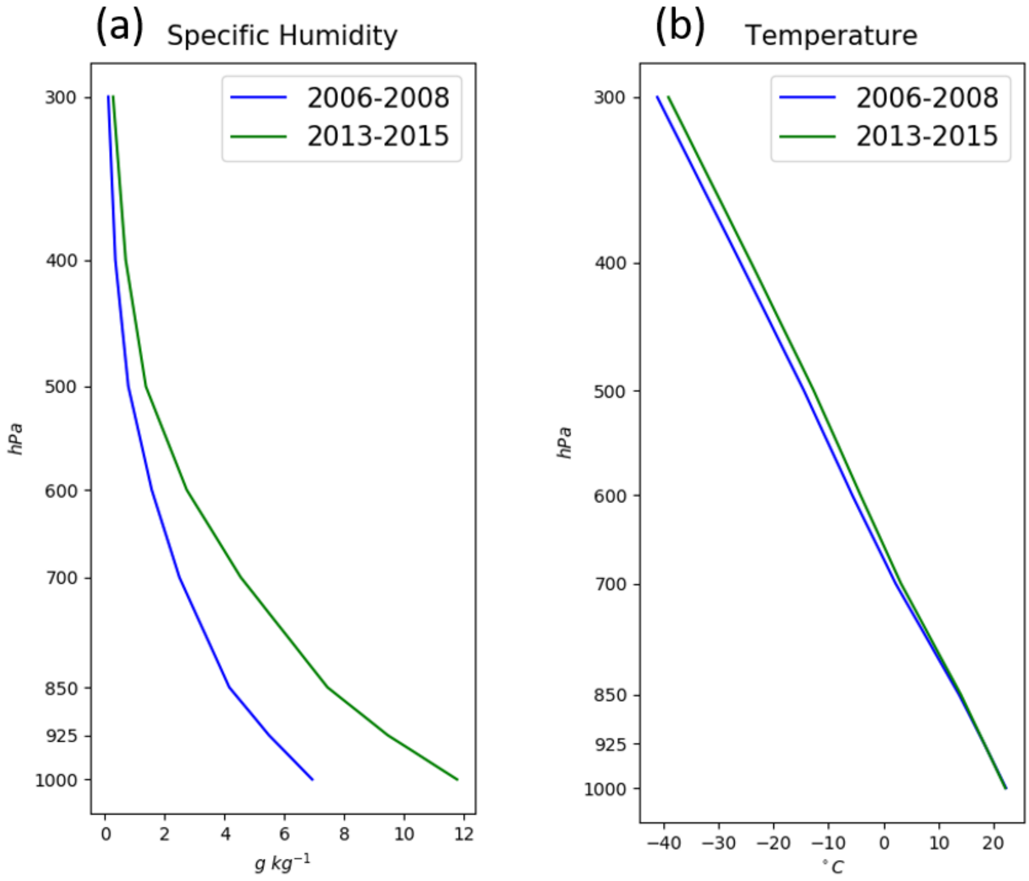

Figure 10 The vertical profile of specific humidity (a) and temperature (b) averaged up the EMP region. The blue lines indicate the averaged value of 3-year period from 2006 to 2008, and the green lines are for 2013 to 2015.

4. Regional climate model simulation

4.1 Model validation of precipitation simulation

The result of WRF model control run was compared with ERA-interim precipitation dataset (fig11~13). The model result showed little bit larger spatial heterogeneity compared to ERA-interim dataset. For large scale precipitation, WRF slightly over simulated the amount and mean bias was 35mm (fig12). On the other hand, WRF significantly over simulated convective precipitation and the mean bias was 99mm (fig13). The mean bias of total precipitation was 134mm (fig11). For all three variables; total, large scale and convective precipitation, even though WRF over simulated the amount of precipitation, the spatial pattern was well simulated and the cosine similarity were 0.987, 0.980, and 0.982 respectively.

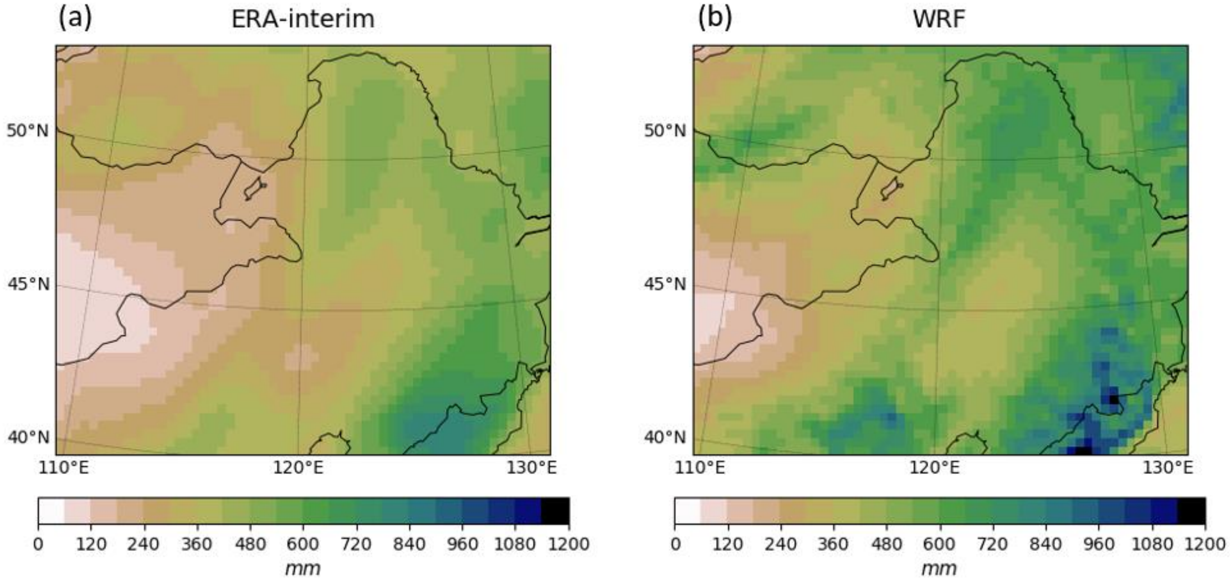

Figure 11 The growing season accumulated total precipitation, averaged from 2007 to 2015, ERA-interim (a) and WRF model simulation result (b). The mean bias (WRF-ERAi) is about 134mm and WRF result showed little bit larger spatial heterogeneity. The overall spatial pattern is reasonable with cosine similarity about 0.986.

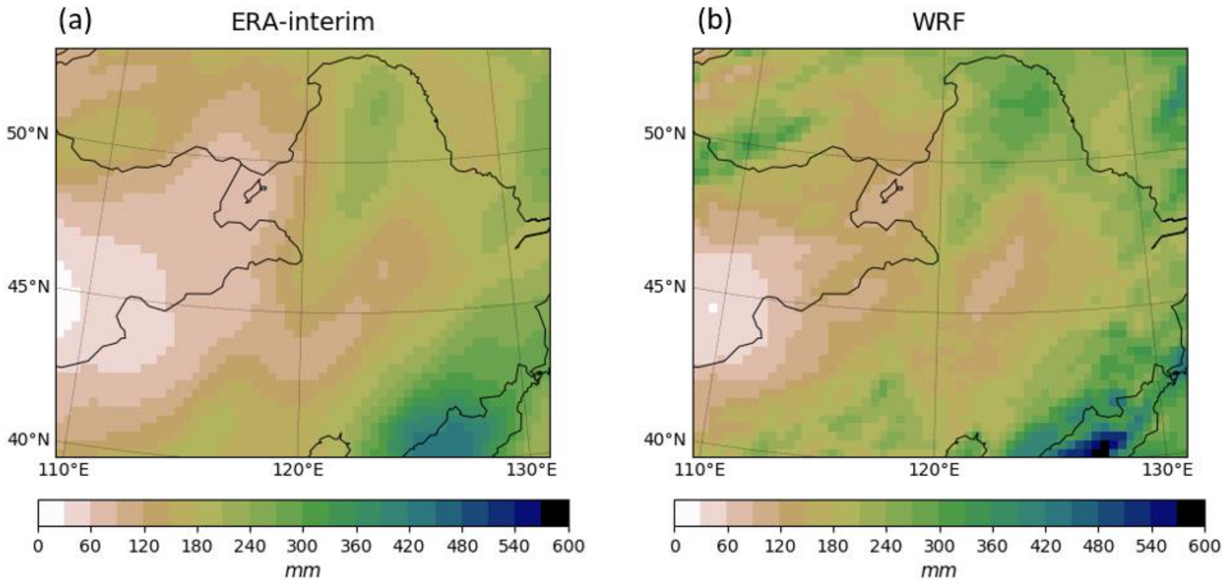

Figure 12 The growing season accumulated large scale precipitation, averaged from 2007 to 2015, ERA-interim (a) and WRF model simulation result (b). The mean bias (WRF-ERAi) is about 35mm. The overall spatial pattern is reasonable with cosine similarity about 0.980.

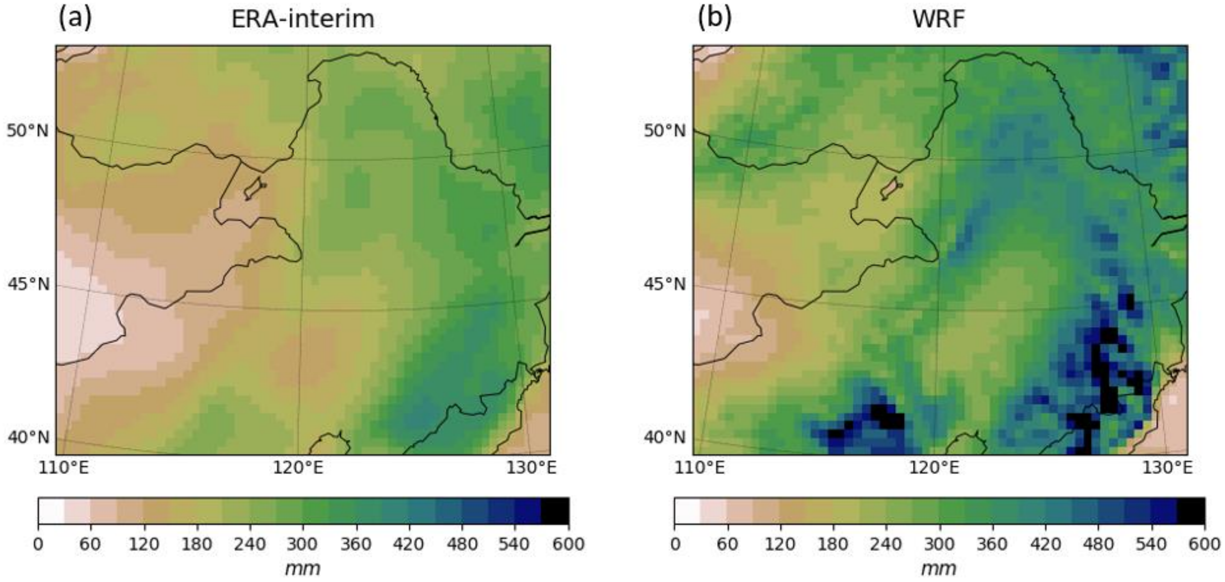

Figure 13 The growing season accumulated convective precipitation, averaged from 2007 to 2015, ERA-interim (a) and WRF model simulation result (b). The mean bias (WRF-ERAi) is about 99mm. In spite of the over simulation, the spatial pattern is reasonable with cosine similarity about 0.982.

4.2 Result of model experiment with modified vegetation activity

Both control and experiment run showed increased latent heat flux at the surface in EMP region. However, the result from control run which consider the effect of vegetation change showed much larger increase than experimental run without considering the effect of vegetation. Thus, in EMP region, the amount of evapo-transpiration has been increased recently and it was partly due to the increase of vegetation activity (fig14). The large scale precipitation also showed increasing trend in EMP region in both control and experimental run, and the control result showed slightly stronger increase (fig15). On the other hand, the convective precipitation showed increasing trend not inside the EMP region but on the boundary of EMP region. Also, the difference between control run and experimental run was very small and not consistent along the boundary (fig16). Overall, the recent increasing trend of precipitation in EMP region seems to be mainly due to the increase of large scale precipitation and increased vegetation activity reinforced the trend.

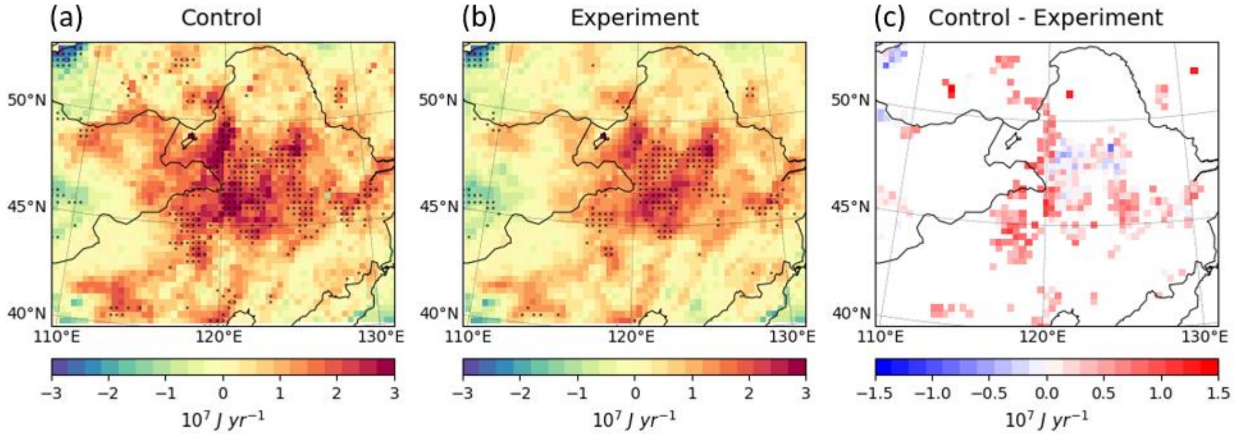

Figure 14 Linear trend of growing season accumulated latent heat flux at the surface of control run (a), experimental run (b) and the difference (c). Experimental run only considers the change due to background meteorological field, without the effect of vegetation, so (c) shows the amount of effect from vegetation change.

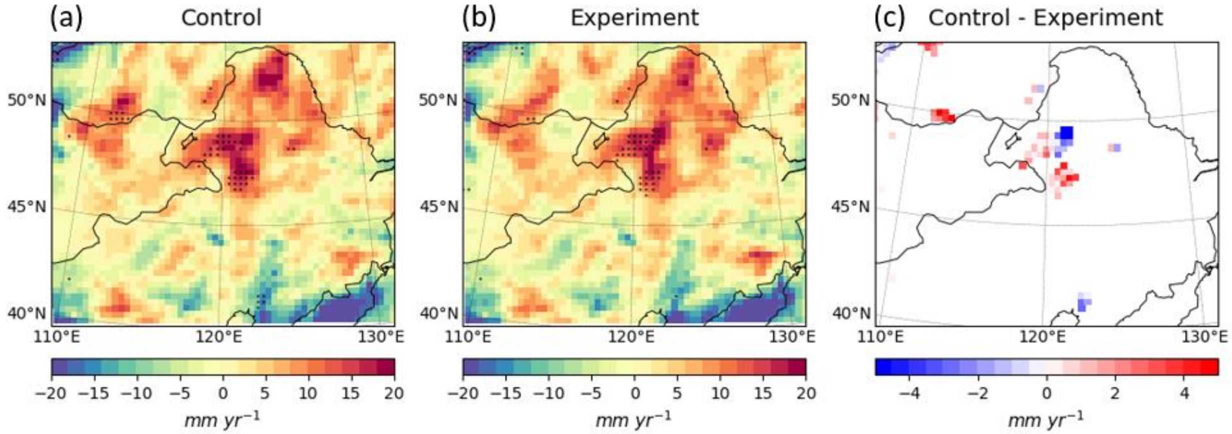

Figure 15 Linear trend of growing season accumulated large scale precipitation of control run (a), experimental run (b) and the difference (c). Experimental run considers the change of precipitation only due to background meteorological field, without the effect of vegetation, so (c) shows the amount of effect from vegetation change.

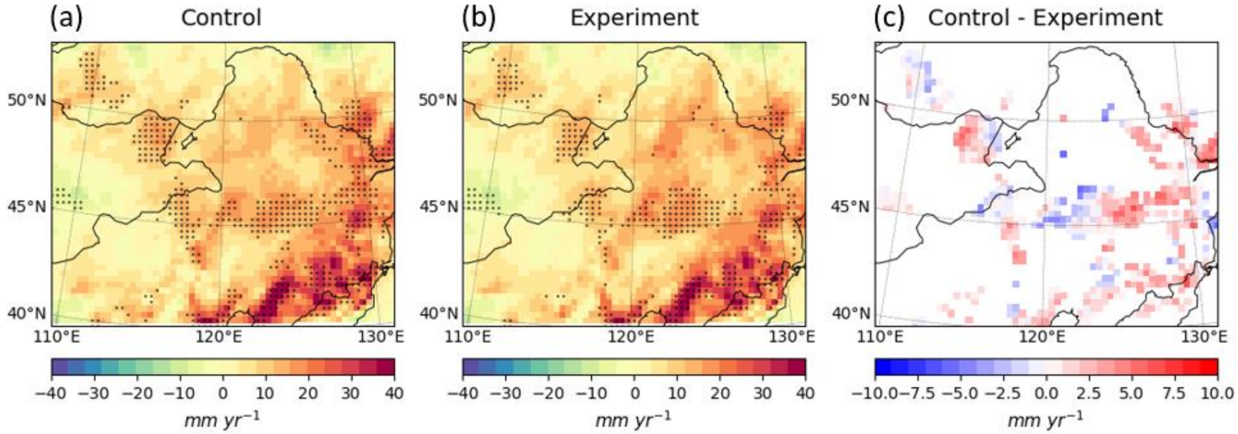

Figure 16 Linear trend of growing season accumulated convective precipitation of control run (a), experimental run (b) and the difference (c). Experimental run considers the change of precipitation only due to background meteorological field, without the effect of vegetation, so (c) shows the amount of effect from vegetation change.

5. Concluding remarks

Increased trend of growing season precipitation and vegetation activity was observed in the EMP region. However, analysis using observation-based reanalysis dataset showed no significant large-scale meteorological field changes that can lead to increased precipitation. Experiments using WRF model have shown that changes in vegetation activity have increased precipitation by increasing the moisture supply to the lower atmosphere via transpiration.

For vegetation, the most significant and strongest increasing trend has been observed at eastern most part of Mongolia, centered around 115°E. However, in case of precipitation, the center is around 120°E, a little bit eastward of vegetation. This area is belonged to the westerly zone. Also, geographically, the altitude of west is higher. If the primary driving force of recent increasing trend was precipitation and the vegetation was simply a consequence, the mechanism of westward affection of increased precipitation is hardly explained. It is much more reasonable to interpret that the increased moisture fluxes from land surface to the atmosphere due to increased vegetation affected on precipitation along the westerly wind. This eastward tilting can also be a evidence of critical role of vegetation feedback and it can be verified if further research is conducted using a back trajectory model.

The EMP region is an artificially afforested area during the 2000s (Shan, Shi, Yang, Gao, & Cai, 2015; Thompson & Clark, 2006). Thus, there are both possibilities that precipitation and vegetation have been reinforcing each other or only the increased vegetation activity due to afforestation has been led the precipitation increase in one-way effect and the precipitation has done nothing on vegetation activity. If a further study is conducted with coupled earth system model focusing on the change of composition of plant functional type, for example the ratio of woody plant and herbaceous plant, it will be possible to make clear which hypothesis is more suitable for recent changes on the EMP region.

Reference

Alkama, R., & Cescatti, A. (2016). Biophysical climate impacts of recent changes in global forest cover. *Science*, *351*(6273), 600–604. https://doi.org/10.1126/SCIENCE.AAC8083

Bonan, G. B. (2008). Forests and Climate Change : Climate Benefits of Forests. *Science*, *320*(June), 1444–1449.

Dee, D. P., Uppala, S. M., Simmons, A. J., Berrisford, P., Poli, P., Kobayashi, S., … Vitart, F. (2011). The ERA-Interim reanalysis: configuration and performance of the data assimilation system. *Quarterly Journal of the Royal Meteorological Society*, *137*(656), 553–597. https://doi.org/10.1002/qj.828

Elmendorf, S. C., Henry, G. H. R., Hollister, R. D., Björk, R. G., Bjorkman, A. D., Callaghan, T. V., … Wookey, P. A. (2012). Global assessment of experimental climate warming on tundra vegetation: Heterogeneity over space and time. *Ecology Letters*, *15*(2), 164–175. https://doi.org/10.1111/j.1461-0248.2011.01716.x

Henninger, N. (2002). *AN ECOSYSTEM APPROACH TO DRYLANDS: Building Support for New Development Policies*. Retrieved from www.wri.org

Huang, J., Guan, X., & Wang, G. (2015). *Accelerated dryland expansion under* *climate change*. https://doi.org/10.1038/nclimate2837

Jeong, S.-J., Ho, C.-H., Brown, M. E., Kug, J.-S., & Piao, S. (2011). Browning in desert boundaries in Asia in recent decades. *Journal of Geophysical Research*, *116*(D2), D02103. https://doi.org/10.1029/2010JD014633

Jeong, S. J., Ho, C. H., Piao, S., Kim, J., Ciais, P., Lee, Y. B., … Park, S. K. (2014). Effects of double cropping on summer climate of the North China Plain and neighbouring regions. *Nature Climate Change*, *4*(7), 615–619. https://doi.org/10.1038/nclimate2266

Kalnay, E., Kanamitsu, M., Kistler, R., Collins, W., Deaven, D., Gandin, L., … Joseph, D. (1996). The NCEP/NCAR 40-Year Reanalysis Project. *Bulletin of the American Meteorological Society*, *77*(3), 437–471. https://doi.org/10.1175/1520-0477(1996)077<0437:TNYRP>2.0.CO;2

Lemordant, L., Gentine, P., Swann, A. S., Cook, B. I., & Scheff, J. (2018). Critical impact of vegetation physiology on the continental hydrologic cycle in response to increasing CO 2 . *Proceedings of the National Academy of Sciences*, *115*(16), 4093–4098. https://doi.org/10.1073/pnas.1720712115

Los, S. O., Weedon, G. P., North, P. R. J., Kaduk, J. D., Taylor, C. M., & Cox, P. M. (2006). An observation-based estimate of the strength of rainfallvegetation interactions in the Sahel. *Geophysical Research Letters*, *33*(16), L16402. https://doi.org/10.1029/2006GL027065

Myers-Smith, I. H., Forbes, B. C., Wilmking, M., Hallinger, M., Lantz, T., Blok, D., … S, R. P. and B. (2011). Shrub expansion in tundra ecosystems: dynamics, impacts and research priorities. *Environmental Research Letters*, *6*(4), 045509. https://doi.org/10.1088/1748-9326/6/4/045509

Ollinger, S. V, Richardson, A. D., Martin, M. E., Hollinger, D. Y., Frolking, S. E., Reich, P. B., … Schmid, H. P. (2008). Canopy nitrogen, carbon assimilation, and albedo in temperate and boreal forests: Functional relations and potential climate feedbacks. *Proceedings of the National Academy of Sciences of the United States of America*, *105*(49), 19336–19341. https://doi.org/10.1073/pnas.0810021105

Park, C.-E., Jeong, S.-J., Joshi, M., Osborn, T. J., Ho, C.-H., Piao, S., … Feng, S. (2017). *Keeping global warming within 1.5 °C constrains emergence of aridification*. https://doi.org/10.1038/s41558-017-0034-4

Richardson, A. D., Keenan, T. F., Migliavacca, M., Ryu, Y., Sonnentag, O., & Toomey, M. (2013). Climate change, phenology, and phenological control of vegetation feedbacks to the climate system. *Agricultural and Forest Meteorology*, *169*, 156–173.

https://doi.org/10.1016/J.AGRFORMET.2012.09.012

Ridder, K. D. E. (1998). the Impact of Vegetation Cover on Sahelian Drought Persistence. *Boundary-Layer Meteorology*, *88*(April), 307–321.

Scheffer, M., Holmgren, M., Brovkin, V., & Claussen, M. (2005). Synergy between small- and large-scale feedbacks of vegetation on the water cycle. *Global Change Biology*, *11*(7), 1003–1012. https://doi.org/10.1111/j.1365-2486.2005.00962.x

Shan, N., Shi, Z., Yang, X., Gao, J., & Cai, D. (2015). Spatiotemporal trends of reference evapotranspiration and its driving factors in the Beijing–Tianjin Sand Source Control Project Region, China. *Agricultural and Forest Meteorology*, *200*, 322–333. https://doi.org/10.1016/J.AGRFORMET.2014.10.008

Thompson, R., & Clark, R. M. (2006). Spatio-temporal modelling and assessment of within-species phenological variability using thermal time methods. *International Journal of Biometeorology*, *50*(5), 312–322. https://doi.org/10.1007/s00484-005-0017-4

Tucker, C. J., Pinzon, J. E., Brown, M. E., Slayback, D. A., Pak, E. W., Mahoney, R., … El Saleous, N. (2005). An extended AVHRR 8-km NDVI dataset compatible with MODIS and SPOT vegetation NDVI data. *International Journal of Remote Sensing*, *26*(20), 4485–4498. https://doi.org/10.1080/01431160500168686

Xie, P., Arkin, P. A., Xie, P., & Arkin, P. A. (1997). Global Precipitation: A 17-Year Monthly Analysis Based on Gauge Observations, Satellite Estimates, and Numerical Model Outputs. *Bulletin of the American Meteorological Society*, *78*(11), 2539–2558. https://doi.org/10.1175/1520-0477(1997)078<2539:GPAYMA>2.0.CO;2

Zhao, X., Hu, H., Shen, H., Zhou, D., Zhou, L., Myneni, R. B., & Fang, J. (2015). Satellite-indicated long-term vegetation changes and their drivers on the Mongolian Plateau. *Landscape Ecology*, *30*(9), 1599–1611. https://doi.org/10.1007/s10980-014-0095-y

국문 초록

식생 피드백은 기후 변화 예측 연구에서 큰 불확실성을 만들어 내는 요소들 중 하나이다. 과거에는 식생의 피드백에 관한 연구가 주로 산림 지역에 초점을 맞추어 이루어졌으며, 지표의 40%를 차지하는 건조 지역을 비롯한 비 산림 지역의 식생피드백은 충분히 연구되지 않았다. 미래의 기후 변화를 정확하게 예측하기 위해서는 건조 지역에서 일어나는 식생 피드백에 대한 연구가 필요하다. 건조 지역에서는 강수와 토양 수분이 밀접하게 연결되어 있으며 식생은 이 연결의 강도를 조절한다. 식생 활동과 강수량은 지역과 시기, 또는 초기 섭동의 크기에 따라 양의 피드백 또는 음의 피드백을 형성할 수 있다. 따라서 개별 사례를 중심으로 연구를 진행 할 필요가 있다. 이 논문에서는 관측 자료와 재분석 자료를 이용한 통계 분석 및 지역 기후 모형 실험을 통하여 2007년부터 2015년까지 관측 된 몽골 고원 동부 지역의 강수량 증가 추세에 식생 피드백이 어떠한 역할을 하였는지 검증하였다.

몽골 고원 동부에서는 2007 년부터 2015 년까지의 기간 동안, 정규 식생 지수가 지난 30년간의 평균값 대비 약 40 % 증가했으며, 같은 기간 강수량은 약 60 % 증가했다. 앞서 이 현상에 대해 논의했던

연구자들은 대기장 변화에 의해 증가 한 강수량이 식생 활동을 증가시켰다고 주장했다. 그러나 2007년부터 2015년까지 외부에서 몽골 고원 동부로 유입되는 수분의 양은 증가하지 않았으며, 기온과 기압 등 주요 대기 변수를 확인해 보았을 때도 강수량 증가를 이끌 만한 유의미한 변화는 관측 되지 않았다. 한편, 2007년부터 2015년까지 하층 대기의 습윤 정적 안정도가 유의미하게 감소한 것을 확인하였는데, 같은 기간 건조 정적 안정도는 유의미한 변화를 보이지 않았다. 건조 정적 안정도와 습윤 정적 안정도는 지난 50년간 장주기 변동성에서 항상 비슷한 추세를 보여왔는데, 2000년대 중반을 기점으로 서로 다른 추세를 보이기 시작하였다. 이는 식생 활동에 의한 증발산이 증가하여 지표에서 하층 대기로의 수분이 증가했기 때문이라고 생각되었다.

지역 기후 모형인 WRF 모형을 사용하여 몽골 고원 동부 지역의 물 순환을 개별 요소로 분해하여 살펴보았을 때, 최근의 강수량 증가 추세의 주된 원인은 대기의 대류 운동 변화보다는 지표로부터의 수분 공급이 증가했기 때문인 것으로 나타났다. 또한 잎 면적 지수(LAI)를 식생 활동이 가장 저조했던 2007년의 값으로 고정하여 식생의 영향을 제거하고 배경 대기장의 변화만을 고려하여 2007년부터 2015년까지

의 강수량 변화를 모의하는 실험을 수행하였을 때 지표로부터 대기로 이동하는 잠열의 증가 추세가 현저하게 감소되며 강수량 증가 추세 또한 감소하는 것으로 나타났다.

관측 자료 분석과 지역 기후 모형 실험의 결과를 종합적으로 고려하면, 몽골 고원의 동부 지역에서 최근 관측 된 강수량 증가에는 식생의 피드백이 중요한 역할을 하였다고 결론 짓는 것이 합리적이다. 대규모 순환의 변화가 강수량 증가를 이끌었다는 증거는 발견되지 않았으며, 지표면에서 대기 중으로 수분 공급이 증가한 것을 확인했다. 또한 지역 기후 모형의 결과는 하층 대기로의 수분 공급의 증가 추세가 주로 식생에 활동에 의한 증산량의 증가로 인한 것으로 나타났다. 전체적인 메커니즘은 2007년부터 2015년까지 식생 활동의 꾸준한 증가로 증산량이 증가했으며, 하층 대기로 공급 되는 수분의 양이 증가하여 국지 강수량이 증가한 것이다.

주요어 : 기후 시스템, 대기-식생 피드백, 건조 지역, 몽골 고원, 강수, 증산 작용

학 번 : 2016-20411